



# Measurement of Natural Widths of $\Sigma_c^0$ and $\Sigma_c^{++}$ Baryons

The FOCUS Collaboration

J. M. Link<sup>a</sup> M. Reyes<sup>a</sup> P. M. Yager<sup>a</sup> J. C. Anjos<sup>b</sup> I. Bediaga<sup>b</sup>  
 C. Göbel<sup>b</sup> J. Magnin<sup>b</sup> A. Massafferri<sup>b</sup> J. M. de Miranda<sup>b</sup>  
 I. M. Pepe<sup>b</sup> A. C. dos Reis<sup>b</sup> S. Carrillo<sup>c</sup> E. Casimiro<sup>c</sup>  
 E. Cuautle<sup>c</sup> A. Sánchez-Hernández<sup>c</sup> C. Uribe<sup>c</sup> F. Vázquez<sup>c</sup>  
 L. Agostino<sup>d</sup> L. Cinquini<sup>d</sup> J. P. Cumalat<sup>d</sup> B. O'Reilly<sup>d</sup>  
 J. E. Ramirez<sup>d</sup> I. Segoni<sup>d</sup> J. N. Butler<sup>e</sup> H. W. K. Cheung<sup>e</sup>  
 G. Chiodini<sup>e</sup> I. Gaines<sup>e</sup> P. H. Garbincius<sup>e</sup> L. A. Garren<sup>e</sup>  
 E. Gottschalk<sup>e</sup> P. H. Kasper<sup>e</sup> A. E. Kreymer<sup>e</sup> R. Kutsche<sup>e</sup>  
 S. Bianco<sup>f</sup> F. L. Fabbri<sup>f</sup> A. Zallo<sup>f</sup> C. Cawfield<sup>g</sup> D. Y. Kim<sup>g</sup>  
 A. Rahimi<sup>g</sup> J. Wiss<sup>g</sup> R. Gardner<sup>h</sup> A. Kryemadhi<sup>h</sup>  
 Y. S. Chung<sup>i</sup> J. S. Kang<sup>i</sup> B. R. Ko<sup>i</sup> J. W. Kwak<sup>i</sup> K. B. Lee<sup>i</sup>  
 H. Park<sup>i</sup> G. Alimonti<sup>j</sup> S. Barberis<sup>j</sup> M. Boschini<sup>j</sup> P. D'Angelo<sup>j</sup>  
 M. DiCorato<sup>j</sup> P. Dini<sup>j</sup> L. Edera<sup>j</sup> S. Erba<sup>j</sup> M. Giammarchi<sup>j</sup>  
 P. Inzani<sup>j</sup> F. Leveraro<sup>j</sup> S. Malvezzi<sup>j</sup> D. Menasce<sup>j</sup> M. Mezzadri<sup>j</sup>  
 L. Milazzo<sup>j</sup> L. Moroni<sup>j</sup> D. Pedrini<sup>j</sup> C. Pontoglio<sup>j</sup> F. Prelz<sup>j</sup>  
 M. Rovere<sup>j</sup> S. Sala<sup>j</sup> T. F. Davenport III<sup>k</sup> V. Arena<sup>l</sup> G. Boca<sup>l</sup>  
 G. Bonomi<sup>l</sup> G. Gianini<sup>l</sup> G. Liguori<sup>l</sup> M. M. Merlo<sup>l</sup> D. Pantea<sup>l</sup>  
 S. P. Ratti<sup>l</sup> C. Riccardi<sup>l</sup> P. Vitulo<sup>l</sup> H. Hernandez<sup>m</sup>  
 A. M. Lopez<sup>m</sup> H. Mendez<sup>m</sup> L. Mendez<sup>m</sup> E. Montiel<sup>m</sup>  
 D. Olaya<sup>m</sup> A. Paris<sup>m</sup> J. Quinones<sup>m</sup> C. Rivera<sup>m</sup> W. Xiong<sup>m</sup>  
 Y. Zhang<sup>m</sup> J. R. Wilson<sup>n</sup> K. Cho<sup>o</sup> T. Handler<sup>o</sup> R. Mitchell<sup>o</sup>  
 D. Engh<sup>p</sup> M. Hosack<sup>p</sup> W. E. Johns<sup>p</sup> M. Nehring<sup>p</sup>  
 P. D. Sheldon<sup>p</sup> K. Stenson<sup>p</sup> E. W. Vaandering<sup>p</sup> M. Webster<sup>p</sup>  
 M. Sheaff<sup>q</sup>

<sup>a</sup>University of California, Davis, CA 95616

<sup>b</sup>Centro Brasileiro de Pesquisas Físicas, Rio de Janeiro, RJ, Brasil

<sup>c</sup>CINVESTAV, 07000 México City, DF, Mexico

<sup>d</sup>University of Colorado, Boulder, CO 80309

<sup>e</sup>Fermi National Accelerator Laboratory, Batavia, IL 60510

<sup>f</sup>*Laboratori Nazionali di Frascati dell'INFN, Frascati, Italy I-00044*

<sup>g</sup>*University of Illinois, Urbana-Champaign, IL 61801*

<sup>h</sup>*Indiana University, Bloomington, IN 47405*

<sup>i</sup>*Korea University, Seoul, Korea 136-701*

<sup>j</sup>*INFN and University of Milano, Milano, Italy*

<sup>k</sup>*University of North Carolina, Asheville, NC 28804*

<sup>l</sup>*Dipartimento di Fisica Nucleare e Teorica and INFN, Pavia, Italy*

<sup>m</sup>*University of Puerto Rico, Mayaguez, PR 00681*

<sup>n</sup>*University of South Carolina, Columbia, SC 29208*

<sup>o</sup>*University of Tennessee, Knoxville, TN 37996*

<sup>p</sup>*Vanderbilt University, Nashville, TN 37235*

<sup>q</sup>*University of Wisconsin, Madison, WI 53706*

See <http://www-focus.fnal.gov/authors.html> for additional author information

---

## Abstract

In this paper we present a measurement of the natural widths of  $\Sigma_c^0$  and  $\Sigma_c^{++}$ . Using data from the FOCUS experiment, we find  $\Gamma(\Sigma_c^0) = 1.55_{-0.37}^{+0.41} \pm 0.38 \text{ MeV}/c^2$  and  $\Gamma(\Sigma_c^{++}) = 2.05_{-0.38}^{+0.41} \pm 0.38 \text{ MeV}/c^2$ . The first errors are statistical, the second systematic. These results are obtained with a sample of 913  $\Sigma_c^0 \rightarrow \Lambda_c^+ \pi^-$  decays and 1110  $\Sigma_c^{++} \rightarrow \Lambda_c^+ \pi^+$  decays. These results are compared with recent theoretical predictions.

PACS numbers: 14.20.Lq 13.30.Eg

---

The natural widths of the excited charmed baryons have become experimentally accessible [1–3] only in the last several years. The widths of most of the known excited charmed baryons are poorly determined with either no existing measurement or with an upper limit;<sup>1</sup> most of the lower mass excited states appear to have widths comparable to or less than the resolution of current experiments. Combined with relatively low statistics, this has made such measurements challenging. Direct measurements of the  $\Sigma_c$  widths are important since most of the current theoretical models predict the widths of charmed baryons by extrapolating from the hyperon widths. Accurate measurements of the  $\Sigma_c$  widths will enable more accurate predictions of the widths of these and other excited charm states and test the physics underlying these models.

In this paper, we use data from the FOCUS experiment to obtain measure-

---

<sup>1</sup> During final preparation of this manuscript, we became aware of a measurement of  $\Sigma_c^0$  and  $\Sigma_c^{++}$  intrinsic widths by the CLEO collaboration [4].

ments of  $\Gamma(\Sigma_c^0)$  and  $\Gamma(\Sigma_c^{++})$ . The  $\Sigma_c^0$  and  $\Sigma_c^{++}$  mass differences with respect to the  $\Lambda_c^+$  were presented in an earlier paper [5]. FOCUS is an upgraded version of FNAL-E687 [6] which collected data using the Wideband photon beamline during the 1996–1997 Fermilab fixed-target run. The FOCUS experiment utilizes a forward multiparticle spectrometer to study charmed particles produced by the interaction of high energy photons ( $\langle E \rangle \approx 180$  GeV) with a segmented BeO target.

Charged particles are tracked within the spectrometer by two silicon microvertex detector systems. One system is interleaved with the target segments; the other is downstream of the target region. These detectors provide excellent separation of the production and decay vertices. Further downstream, charged particles are tracked and momentum analyzed by a system of five multiwire proportional chambers and two dipole magnets with opposite polarity. Three multicell threshold Čerenkov detectors are used to discriminate among electrons, pions, kaons, and protons [7].

The  $\Sigma_c$  candidates are reconstructed via the decay chain  $\Sigma_c \rightarrow \Lambda_c^+ \pi^\pm$ , with  $\Lambda_c^+$  candidates found in four decay modes,<sup>2</sup>  $\Lambda_c^+ \rightarrow pK^-\pi^+$ ,  $pK_S^0$ ,  $\Lambda^0\pi^+$ , and  $\Lambda^0\pi^+\pi^-\pi^+$ . The reconstruction of  $K_S^0$ 's and  $\Lambda^0$ 's is described elsewhere [8]. Due to topological differences and varying levels of background, the values of the analysis cuts for each of the four  $\Lambda_c^+$  decay modes vary. A decay, or secondary, vertex is formed from selected reconstructed tracks; the momentum vector of this charm candidate is then used as a seed to intersect other reconstructed tracks in the event to find the production, or primary, vertex [6]. We impose a minimum detachment cut which requires that the measured separation of these two vertices divided by the error on that measurement be greater than our cut (typically 3–5). We also ensure that both vertices are well formed by requiring a confidence level greater than 1% on the fit to each vertex. To remove longer lived charm backgrounds we also require the reconstructed proper lifetime to be less than some amount, typically 4–5 times the mean  $\Lambda_c^+$  lifetime. Finally, momentum and particle identification cuts are applied to each decay mode. Invariant mass plots for each of the decay modes are shown in Fig. 1.

The  $\Sigma_c$  candidates are reconstructed by combining the  $\Lambda_c^+$  candidates within approximately  $2\sigma$  of the mean  $\Lambda_c^+$  mass with a charged pion.<sup>3</sup> The vertex formed by the  $\Lambda_c^+$  candidate, the pion candidate, and at least one other track must have a confidence level greater than 1%. Čerenkov identification on the soft pion requires that the pion hypothesis is not heavily disfavored with respect to any other identification hypothesis.

To remove systematic effects due to the reconstruction of the  $\Lambda_c^+$  mass, we

<sup>2</sup> Throughout, charge conjugate states are implied.

<sup>3</sup> Referred to as a “soft pion” since it is usually a low momentum particle.

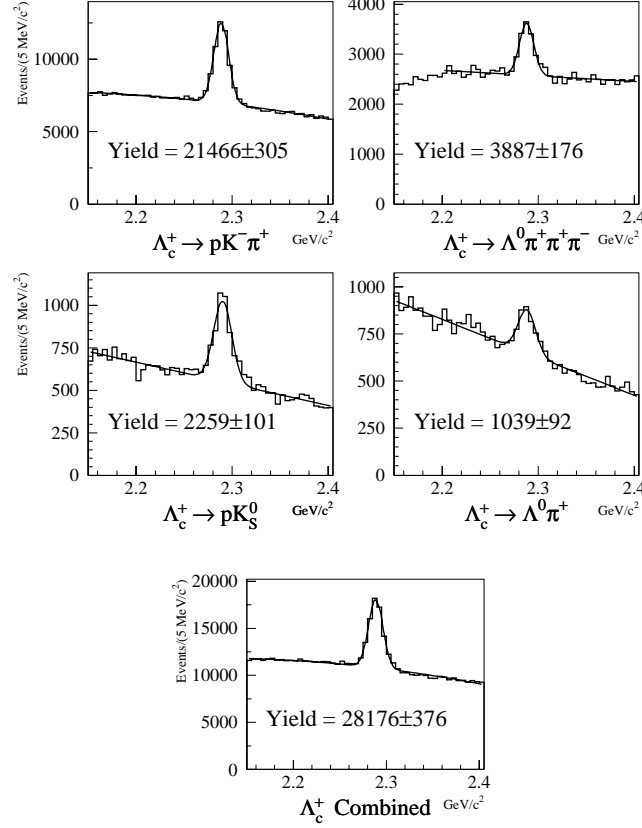


Fig. 1. Invariant mass distributions for  $\Lambda_c^+$  candidates. Shown are the four  $\Lambda_c^+$  decay modes used in the analysis and, on the bottom, the combined invariant mass plot for all four decay modes.

compute and plot the invariant mass differences ( $\Delta M = M(\Lambda_c^+ \pi^\pm) - M(\Lambda_c^+)$ ). Because most of the uncertainty in the mass difference arises due to multiple scattering of the soft pion, we improve the measurement of the soft pion momentum as follows. The primary vertex is refit without the soft pion and the soft pion is constrained to originate from this new primary vertex. If the confidence level of this constraint is less than 1%, the candidate is discarded. The measured  $\Lambda_c^+$  momentum and mass are combined with the constrained pion momentum and known mass to form  $M(\Lambda_c^+ \pi^\pm)$ . The computed  $\Lambda_c^+$  mass is subtracted to obtain the invariant mass difference,  $\Delta M$ . The reconstructed mass difference distributions are shown in Fig. 2.

To measure  $\Gamma(\Sigma_c)$ , we fit the  $\Sigma_c$  signal distributions with a relativistic constant width Breit–Wigner function convoluted with a parameterization of the experimental resolution derived from Monte Carlo. The experimental resolution is determined by generating Monte Carlo events with  $\Gamma(\Sigma_c) = 0$  and fitting the resulting  $\Sigma_c$  distributions to a sum of two Gaussians,  $G(x; \text{Yield}, \sigma, \bar{x})$ , with the same central value  $\bar{x}$ :

$$G(\Delta M; (1-f)Y, \sigma_1, M_{\text{fit}}) + G(\Delta M; fY, \sigma_2, M_{\text{fit}}) . \quad (1)$$

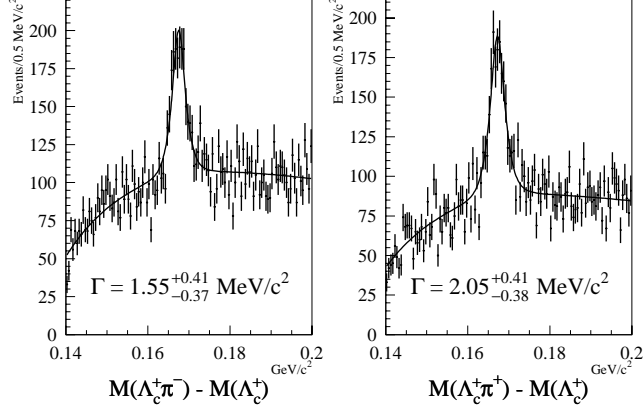


Fig. 2. Invariant mass differences for  $\Sigma_c^0$  (left) and  $\Sigma_c^{++}$  (right) candidates. The fit functions, over their range of 140–200  $\text{MeV}/c^2$ , are shown as are the widths and statistical errors.

Table 1

$\Sigma_c$  resolution parameters calculated in Monte Carlo.

State	$\sigma_1$ ( $\text{MeV}/c^2$ )	$\sigma_2$ ( $\text{MeV}/c^2$ )	$f$ Yield <sub>2</sub> /(Yield <sub>1</sub> + Yield <sub>2</sub> )
$\Sigma_c^0$	$0.84 \pm 0.03$	$1.93 \pm 0.05$	$0.53 \pm 0.03$
$\Sigma_c^{++}$	$0.83 \pm 0.03$	$1.92 \pm 0.05$	$0.56 \pm 0.03$

We use a background function described by

$$N(1 + \alpha(\Delta M - m_\pi)\Delta M^\beta) \quad (2)$$

where  $m_\pi$  is the  $\pi^\pm$  mass.  $N$ ,  $\alpha$ , and  $\beta$  are allowed to vary. Three parameters of interest are extracted from the fit:  $\sigma_1$ ,  $\sigma_2$ , and  $f = Y_2/Y$  which describe, respectively, the resolution of the narrow and wide portions of the resolution function and the ratio of the second yield to the total.  $M_{\text{fit}}$  is the  $\Sigma_c - \Lambda_c^+$  mass difference.

We determine the shape parameters ( $\alpha$  and  $\beta$ ) of the background function (Eq. (2)) by fitting the sum of the  $M(\Lambda_c^+ \pi^+)$  and the  $M(\Lambda_c^+ \pi^-)$  data distributions to Eq. (2) and a convoluted Breit–Wigner signal shape. The values of  $\alpha$  and  $\beta$  are fixed to these values when fitting the individual distributions.

While the fits for  $\Sigma_c^0$  and  $\Sigma_c^{++}$  distributions to a Breit–Wigner convoluted with the resolution function use a total of nine parameters, only four of these are free parameters (yield,  $M(\Sigma_c - \Lambda_c^+)$ ,  $\Gamma(\Sigma_c)$ , and  $N$ , the background normalization). The parameters  $\alpha$ ,  $\beta$ ,  $\sigma_1$ ,  $\sigma_2$ , and  $f$  are previously determined and are fixed. Performing the fit as described above we obtain values of  $\Gamma(\Sigma_c^0) = 1.55^{+0.41}_{-0.37} \text{ MeV}/c^2$  and  $\Gamma(\Sigma_c^{++}) = 2.05^{+0.41}_{-0.38} \text{ MeV}/c^2$  with yields of  $913 \pm 77$  and  $1110 \pm 83$  respectively. The extracted mass differences are consistent with our previous measurement [5].

Table 2

Comparison of  $D^{*+}$  line shape parameters for data and Monte Carlo. Statistical errors only.

State	$\sigma_1$ (MeV/ $c^2$ )	$\sigma_2$ (MeV/ $c^2$ )	$f$
$D^{*+}$ Data	$0.66 \pm 0.00$	$3.5 \pm 0.2$	$0.05 \pm 0.02$
$D^{*+}$ MC	$0.61 \pm 0.00$	$2.8 \pm 0.5$	$0.05 \pm 0.02$

The largest systematic uncertainties in this measurement arise from our imperfect knowledge of the experimental mass resolution. To better understand our experimental resolution in a kinematically similar situation, we have used the decay  $D^{*+} \rightarrow D^0\pi^+$  as a benchmark. The  $D^{*+}$  is much closer to decay threshold and should expose any problems with our simulation of the experimental resolution. We compare the resolution of classes of events seen in the data with that seen in the simulation. The Monte Carlo uses an input  $D^{*+}$  natural width of 96 keV/ $c^2$ , the value from a recent CLEO [9,10] report. For both Monte Carlo and data we fit the distributions to the sum of Eq. (1) and Eq. (2). No value of  $\Gamma(D^{*+})$  is determined by or included in the fit. (Since  $\Gamma(D^{*+}) \ll \sigma(\Delta M(D^{*+}))$ , the precise value of  $\Gamma(D^{*+})$  influences the fit results only slightly. The Breit–Wigner modifications to the line shape are negligible and are safely ignored.) By studying any discrepancies in the  $D^{*+}$  case, we understand our experimental resolution better for the  $\Sigma_c$ .

We find that for the  $D^{*+}$ , our overall experimental resolution matches that predicted by the Monte Carlo quite well and find no definitive evidence for any discrepancy except for  $\sigma_1$  which is about 10% less in Monte Carlo. The values of the fits to the  $D^{*+}$  line shape for data and Monte Carlo are shown in Table 2. To be conservative, we test the effects of varying the experimental resolution by the maximum allowed by our  $D^{*+}$  studies. In our description of the predicted resolution we independently vary the three parameters  $\sigma_1$ ,  $\sigma_2$ , and  $f$  by  $\pm 10\%$ ,  $\pm 20\%$ , and  $\pm 15\%$  respectively. These changes induce variations of approximately  $\mp 0.20$ ,  $\mp 0.25$ , and  $\mp 0.20$  MeV/ $c^2$  in  $\Gamma(\Sigma_c)$ , respectively.

In addition, we have studied the resolution function for the  $D^{*+}$  as a function of target configurations, the production target segment, decay modes, and the detachment cut. The resolution is clearly dependent on the production target segment and the several target configurations used in FOCUS. The dependence of the resolution on these two variables is well predicted by the Monte Carlo simulation and the distribution of  $\Sigma_c$  events as a function of these variables is also well matched by the Monte Carlo. The resolution function also depends somewhat on the kinematic variables, most strongly on the momentum of the excited state. As an example, in Table 3, we show the variation of  $\sigma_1$  for the  $D^{*+}$  in four bins of momentum. The data and Monte Carlo disagree by less than 10% as shown in Table 2, but the disagreement is constant vs.  $D^{*+}$

Table 3

Comparison of  $D^{*+}$  core resolution,  $\sigma_1$  ( $\text{MeV}/c^2$ ), vs. momentum.

$p(D^{*+})$ $\text{GeV}/c$	< 60	60–80	80–100	> 100
$D^{*+}$ Data	$0.61 \pm 0.01$	$0.63 \pm 0.01$	$0.65 \pm 0.01$	$0.70 \pm 0.01$
$D^{*+}$ MC	$0.57 \pm 0.00$	$0.59 \pm 0.00$	$0.62 \pm 0.00$	$0.66 \pm 0.00$

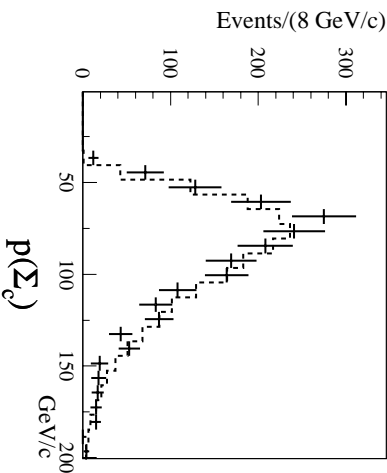


Fig. 3. Momentum spectrum of  $\Sigma_c^0$  and  $\Sigma_c^{++}$  (summed) for data (points) and Monte Carlo (dashed curve). Both Monte Carlo and data are sideband subtracted.

momentum. In Fig. 3, we show that the  $\Sigma_c$  momentum distribution is well modeled by the Monte Carlo. Other variations in resolution are found as a function of soft pion momentum and charm and soft pion directions, with a weaker dependence on these kinematic variables.

We also perform two additional tests of our fitting and reconstruction method. In the first, we produce a large number of distributions which are statistically similar to the data. These distributions are then fit with the same methods used for the real data. The extracted fit parameters are compared with the known input parameters. From this source we estimate a maximum bias in the fitting technique of  $0.05 \text{ MeV}/c^2$  and confirm the validity of our statistical errors.

In the second test, we generate Monte Carlo events with a natural width which is comparable to what is measured and measure the width of these events using the same methods. From this study we find no evidence for a systematic error.

Adding all the systematic errors in quadrature, we find a total systematic error of  $\pm 0.38 \text{ MeV}/c^2$  for each  $\Gamma(\Sigma_c)$  measurement. This gives final values of  $\Gamma(\Sigma_c^0) = 1.55_{-0.37}^{+0.41} \pm 0.38 \text{ MeV}/c^2$  and  $\Gamma(\Sigma_c^{++}) = 2.05_{-0.38}^{+0.41} \pm 0.38 \text{ MeV}/c^2$ .

There are several recent theoretical predictions for the widths of the  $\Sigma_c$  states [11–16]; all predict  $\Gamma(\Sigma_c)$  in the range 1–3  $\text{MeV}/c^2$ . Several different theoretical models are used, including the Relativistic Three Quark Model (RTQM), Heavy Hadron Chiral Perturbation Theory (HHPT), and the Light Front

Table 4

Predicted  $\Sigma_c$  widths from various theoretical models. All units are  $\text{MeV}/c^2$ .

Author	$\Gamma(\Sigma_c^0)$	$\Gamma(\Sigma_c^{++})$	Method
Ivanov, et al. [11,12]	$2.65 \pm 0.19$	$2.85 \pm 0.19$	RTQM
Tawfig, et al. [13]	1.57	1.64	LFQM
Huang, et al. [14]	2.4	2.5	HHCT
Pirjol, et al. [15]	1.0–3.0	1.1–3.1	HHCT
Rosner [16]	$1.32 \pm 0.04$	$1.32 \pm 0.04$	Ratios

Quark Model (LFQM).

These models predict partial widths, but since  $\Sigma_c \rightarrow \Lambda_c^+ \pi$  is the only allowed strong or electromagnetic decay mode for the states under study, we safely take the partial width as the total width for each state. The resulting predictions from the models are shown in Table 4. Our measurements are not of sufficient precision to strongly favor any one of these models over another.

In conclusion, we present measurements of the natural widths of the  $\Sigma_c^0$  and  $\Sigma_c^{++}$  excited charmed baryons using data from the FOCUS experiment. We find  $\Gamma(\Sigma_c^0) = 1.55_{-0.37}^{+0.41} \pm 0.38 \text{ MeV}/c^2$  and  $\Gamma(\Sigma_c^{++}) = 2.05_{-0.38}^{+0.41} \pm 0.38 \text{ MeV}/c^2$  which are consistent with most current theoretical predictions.

We wish to acknowledge the assistance of the staffs of Fermi National Accelerator Laboratory, the INFN of Italy, and the physics departments of the collaborating institutions. This research was supported in part by the U. S. National Science Foundation, the U. S. Department of Energy, the Italian Istituto Nazionale di Fisica Nucleare and Ministero dell’Università e della Ricerca Scientifica e Tecnologica, the Brazilian Conselho Nacional de Desenvolvimento Científico e Tecnológico, CONACyT-México, the Korean Ministry of Education, and the Korean Science and Engineering Foundation.

## References

- [1] H. Albrecht, et al., Evidence for  $\Lambda_c^+(2593)$  production, Phys. Lett. B402 (1997) 207–212.
- [2] K. W. Edwards, et al., Observation of excited baryon states decaying to  $\Lambda_c^+ \pi^+ \pi^-$ , Phys. Rev. Lett. 74 (1995) 3331.
- [3] G. Brandenburg, et al., Observation of two excited charmed baryons decaying into  $\Lambda_c^+ \pi^\pm$ , Phys. Rev. Lett. 78 (1997) 2304–2308.
- [4] M. Artuso, et al., Measurement of the masses and widths of the  $\Sigma_c^{++}$  and  $\Sigma_c^0$  charmed baryons ArXiv:hep-ex/0110071.



- [5] J. M. Link, et al., Measurements of the  $\Sigma_c^0$  and  $\Sigma_c^{++}$  mass splittings, Phys. Lett. B488 (2000) 218–224.
- [6] P. L. Frabetti, et al., Description and performance of the Fermilab E687 spectrometer, Nucl. Instrum. Meth. A320 (1992) 519–547.
- [7] J. M. Link, et al., Čerenkov particle identification in FOCUS ArXiv:hep-ex/0108011, accepted for publication in Nucl. Instr. Meth.
- [8] J. M. Link, et al., Reconstruction of vees, kinks,  $\Xi^-$ 's, and  $\Omega^-$ 's in the FOCUS spectrometer ArXiv:hep-ex/0109028, accepted for publication in Nucl. Instr. Meth.
- [9] S. Ahmed, First measurement of  $\Gamma(D^{*+})$  ArXiv:hep-ex/0108013.
- [10] A. Anastassov, et al., First measurement of  $\Gamma(D^{*+})$  and precision measurement of  $m(D^{*+}) - m(D^0)$  ArXiv:hep-ex/0108043.
- [11] M. A. Ivanov, J. G. Körner, V. E. Lyubovitskij, A. G. Rusetsky, One pion charm baryon transitions in a relativistic three quark model, Phys. Lett. B442 (1998) 435.
- [12] M. A. Ivanov, J. G. Körner, V. E. Lyubovitskij, A. G. Rusetsky, Strong and radiative decays of heavy flavored baryons, Phys. Rev. D60 (1999) 094002.
- [13] S. Tawfiq, P. J. O'Donnell, J. G. Körner, Charmed baryon strong coupling constants in a light front quark model, Phys. Rev. D58 (1998) 054010.
- [14] M.-Q. Huang, Y.-B. Dai, C.-S. Huang, Decays of excited charmed  $\Lambda$ -type and  $\Sigma$ -type baryons in heavy hadron chiral perturbation theory, Phys. Rev. D52 (1995) 3986–3992.
- [15] D. Pirjol, T.-M. Yan, Predictions for s wave and p wave heavy baryons from sum rules and constituent quark model, Phys. Rev. D56 (1997) 5483–5510.
- [16] J. L. Rosner, Charmed baryons with  $J = 3/2$ , Phys. Rev. D52 (1995) 6461–6465.